Article

Not peer-reviewed version

Integrated Application of Geospatial Technologies and UAS-Based Thermal Photogrammetry for Mapping and Assessment of the Surface Urban Heat Island Intensity for Effective Climate Change Adaptation and Sustainable Development of the Urban Areas

Stelioan Slavkov Dimitrov *, Martin Borisov Iliev, Bilyana Bogomilova Borisova, Lidiya Nikolaeva Semerdzhieva, Stefan Stefanov Petrov

Posted Date: 8 January 2024

doi: 10.20944/preprints202401.0613.v1

Keywords: Urban Heat Island (UHI); Surface Urban Heat Island (SUHI); thermal photogrammetry; Unmanned Aerial Systems (UAS); sustainable urban planning

Article

Integrated Application of Geospatial Technologies and UAS-Based Thermal Photogrammetry for Mapping and Assessment of the Surface Urban Heat Island Intensity for Effective Climate Change Adaptation and Sustainable Development of the Urban Areas (a Case Study of Lyulin Housing Complex, Sofia City, Bulgaria)

Stelian Dimitrov [1,*], Martin Iliev [2], Bilyana Borisova [3], Lidiya Semerdzhieva [4] and Stefan Petrov [5]

[1] Sofia University St.Kliment Ohridski; stelian@gea.uni-sofia.bg
[2] Sofia University St.Kliment Ohridski; martin@gea.uni-sofia.bg
[3] Sofia University St.Kliment Ohridski; billiana@gea.uni-sofia.bg
[4] Sofia University St.Kliment Ohridski; l.nikolaeva@gea.uni-sofia.bg
[5] Sofia University St.Kliment Ohridski; s.petrov@gea.uni-sofia.bg
* Correspondence: stelian@gea.uni-sofia.bg

Abstract: The urban heat island (UHI) and its intensity is one of the phenomena that are of determining importance for the comfort of living in cities and their sustainable development in the face of deepening climate change. The study is objectively difficult due to the large dynamics like land cover and the considerable diversity of land use patterns in urban areas. Various approaches and methods are used in research practice, based both on ground measurements and in the use of remote methods and satellite information. However, most of these approaches provide information with problematic spatial and temporal resolution, making them difficult to apply for sustainable urban planning purposes, which require adequate information provision. This paper presents the results of the application of thermal photogrammetry based on the use of unmanned aerial systems (UAS), combined with geographic information systems (GIS), in the study of surface urban heat island intensity (SUHI), at the local level for the largest housing complex in Bulgaria - Lyulin district of the capital of Sofia city. The studies were carried out during a heat wave in July 2023. A difference of 16.5°C was found between locations with SUHI occurrence and suburban areas. The information benefits of locally addressed data and their direct applicability are discussed to support decision-making processes in the planning and management of urban areas, including their climate adaptation and sustainable development.

Keywords: urban heat island (UHI); surface urban heat island (SUHI); thermal photogrammetry; unmanned aerial systems (UAS); sustainable urban planning

1. Introduction

Processes of intensive urbanization is accompanied by a continuous densification of geographical space with artificial surfaces and objects, overconcentration of population, economic and social activities [1]. The combination of these circumstances has a direct impact on the formation of urban climate and on the energy balance of urban climate systems, which is of crucial importance for their sustainable development [2]. The formation and retention of higher temperatures in urban spaces relative to their neighboring areas is defined as the Urban Heat Island effect. Since the first documented research in this area, conducted by Luke Howard in London [3] in the late 19th century, this phenomenon has been studied in a variety of cities of diverse sizes and geographic locations [4-6]. Higher temperatures on the ground surface and in the air in contact are increasing the temperature stress on urban populations, especially during the summer months, which significantly affects total mortality rates [7-8]. Energy costs for cooling are increasing [9], as well as the occurrence of other

 doi:10.20944/preprints202401.0613.v1

environmental problems, related to greenhouse gas and other emissions in the atmosphere [10]. Those effects are likely going to be further exacerbated when considering the deepening of climate change [11-13]. Apart from health risks, the joint economic costs of urban impacts from the UHI effect and climate change have been estimated to be 2.6 times those without the UHI effect [14]. Therefore, measures to reduce the impact of UHI will also contribute to urban heat stress mitigation, especially in the future with more frequent and stronger extreme heat events due to the interactions between urban climate, heat waves, climate change, and urbanization [15]. It is for these reasons that mapping and assessing the urban heat island effect emerges as an important issue in contemporary urban planning.

The UHI is a complex geospatial phenomenon that includes at least three major manifestations: (1) within the surface of the urban area and the immediate subsurface urban heat island (SUHI); (2) the immediate atmospheric layer enveloping the city and the buildings, technical infrastructure, and population included within its boundaries; and (3) the boundary region within the peri-urban space formed along the direction of the prevailing air mass movement [16]. The intensity and timing of UHI are derived from the structural characteristics of urban sites - building in compact forms with dense materials of low permeability and high heat capacity. These patterns of geographic land use change the natural morphology of the terrain to a complex heterogeneous system and form geodynamic and atmospheric processes of different natures. They result in specific climatic regimes with a high degree of spatial variability, significantly different from the thermal, hydrostatic, and radiative properties of natural landscapes. This situation is further complicated by the high concentration of atmospheric pollutants in cities, as well as by anthropogenic thermal emissions into the urban atmosphere, which also contribute synergistically to the formation of artificially created warmer urban spaces.

Intense urbanization in combination with global climate change is likely to lead to an intensification of UHI and the negative consequences of this phenomenon on urban governance, organization and planning, health, and well-being of urban residents [17]. These issues have been a sustained focus of research interest [18-19], with a not insignificant amount of this research emphasizing the need for accurate quantitative and spatial parameterization of UHI intensity and the factors that determine it [20]. Knowledge of the genesis and dynamics of UHI, especially of the SUHI, will contribute to the informed renewal of urban planning approaches and to enhancing the effectiveness of decisions taken to organize sustainable urban environments in the process of accelerated adaptation to climate challenges. Currently, there is a deficit of such research due to the complexity of correctly quantifying the occurrence of UHI and the intensity of the phenomenon in different structural parts of urban spaces [21-23].

Our research is based on the hypothesis that an integrated approach using modern geospatial technologies and Unmanned aerial system (UAS) based thermal photogrammetry can provide quantitative data with high precision and spatial resolution for detailed mapping and assessment of the SUHI. The results of such a combination of urban spatial research methods provide the much-needed quantitative and spatially referenced information for the selection of appropriate short and long-term urban and landscape planning measures to mitigate its effect in an individual approach to a given urban morphostructure. Mapping of the results can be used with the importance of a communication tool with stakeholders. Appropriate visualization can help to integrate this specialized research information into discussion and decision-making in support of sustainable urban management and adaptation to climate change - urban planning of living spaces, health, energy efficiency, and green systems.

This study aims to provide a rationale for the use of an integrated approach for the assessment and mapping of SUHI and its intensity, and to discuss the results of a test of the methodology in a study of the largest housing complex of the Bulgarian capital city of Sofia – Lyulin. This is typical for Eastern European cities' residential complexes with large-scale high-rise housing, combined with impervious areas and unstructured green spaces.

The methodological solutions presented here are directly aimed at facilitating the applicability of the results of SUHI assessment and mapping in plans and procedures for the effective adaptation

Preprints (www.preprints.org) | NOT PEER-REVIEWED | Posted: 8 January 2024 doi:10.20944/preprints202401.0613.v1

of urban areas to deepening climate change and their gradual transformation into sustainable territorial communities.

2. Materials and Methods

2.1. Study area

The subject of the present study is the territory of the housing complex Lyulin, located in the northwestern part of Sofia Municipality (Figure 1). This is the largest residential area in Bulgaria (125 thousand inhabitants, 2023), designed in the 1960s (and built by the mid-1980s) as a relatively self-contained structure with ten micro-districts on an area of 5.7 km^2. It is executed in the style of large-panel construction (about 70%) with a predominance of high-rise residential buildings (over 6 storeys). The layout of the area is strongly influenced by the development of the metropolitan city of Sofia and the dynamic changes in its functioning after the political changes in Eastern Europe in the 1990s. To the west, the district is bounded by the ring road, and to the southeast lies one of the largest urban parks in Sofia - the Western Park. To this day, the planned sports facilities, the main community center, and multi-storey car parks have not been realized.

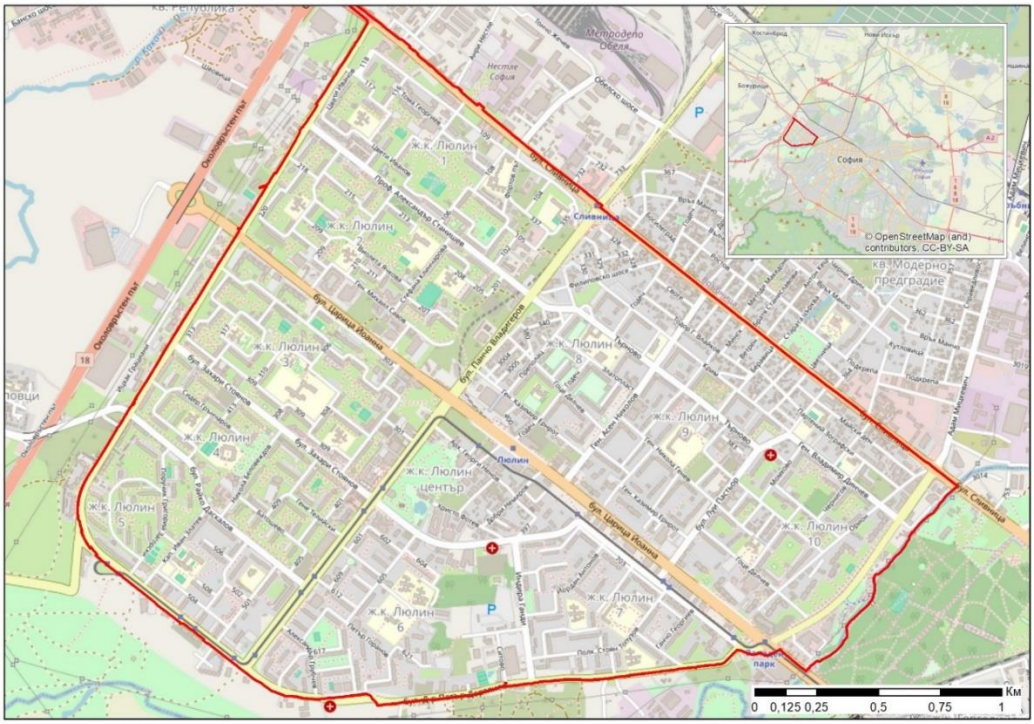

Figure 1. Study area – Lyulin housing complex**.**

55% of the area of Lyulin housing complex is municipally owned and 25% is privately owned. Around 60% of the area is designated for development, 25% is designated for transport infrastructure. There are 3 863 buildings present: the highest number of buildings is 1 to 6 storeys (58 %), buildings with 6 to 10 storeys account for 38 % and high-rise buildings over 11 storeys account for 4 %. There are 52,962 registered freehold properties in buildings, of which over 88% are dwellings and flats [24].

The Lyulin housing complex is the first area in Sofia where the metro line was launched. It is characterized by increased investment interest, both in the construction and real estate markets. The development in the complex is characterized by the creation of characteristic sealed zones between the high-rise residential buildings with a tendency towards a steady absorption of more and more empty spaces, which are filled with industrial, commercial, or residential buildings. This leads to the continuous densification and saturation of the geographical space with artificial surfaces and objects,

Preprints (www.preprints.org) | NOT PEER-REVIEWED | Posted: 8 January 2024 doi:10.20944/preprints202401.0613.v1

the concentration of population, and economic activities. The complex is bisected by two large perpendicular boulevards with a high traffic flow and no substantial landscaping along its length.

The climate of Sofia Municipality is temperate-continental with four seasons, but the regime of climatic elements is strongly influenced by the shape of the Sofia Basin (in which the city of Sofia is located), the altitude (550 m a.s.l.) and the orography of the neighboring chain mountain systems (Srednogorie – Vitosha Mountain, 2291 m and Stara Planina - Sofiyska Mountain, 1294 m). According to meteorological observations (from 1881 to the present), the average annual temperature of Sofia is 10.3°C and the average annual precipitation is 612 mm, with a maximum in May-June. The prevailing air mass movement is from the west-northwest. The average temperature of the coldest month is -1.7°C and of the warmest month 21.2°C. Temperature inversions and pronounced maximum temperatures are common: the measured absolute minimum air temperature is -27,5°C and the absolute maximum temperature is 37,4°C.

The geographic conditions combined with the morphology of Sofia's urban structure create the preconditions for the intense occurrence of the UHI effects [25], combined with the retention of pollutants in the ground air, which is a persistent problem for the management of Sofia Municipality [26]. Data over the period 1979 to 2021 [27] show an increasing trend in mean temperatures, which is particularly clear from 2007 to the present (Figure 2). This is accompanied by more prolonged heat waves, which in the densely urbanized structure of the Lyulin complex increases temperature stress.

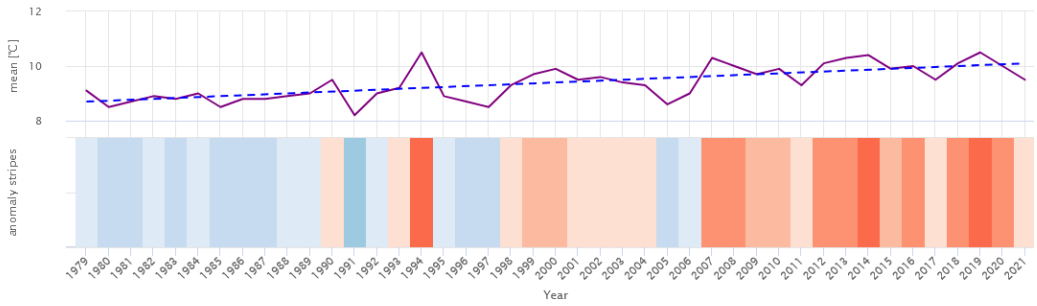

Figure 2. Annual mean temperature change-1979-2022 in the city of Sofia [27].

The frequency of these events is mainly concentrated in the months of July and August, but tends to expand towards June and September (Figure 3). These circumstances will directly affect living conditions in the area and the functioning of infrastructure systems.

Preprints (www.preprints.org) | NOT PEER-REVIEWED | Posted: 8 January 2024 doi:10.20944/preprints202401.0613.v1

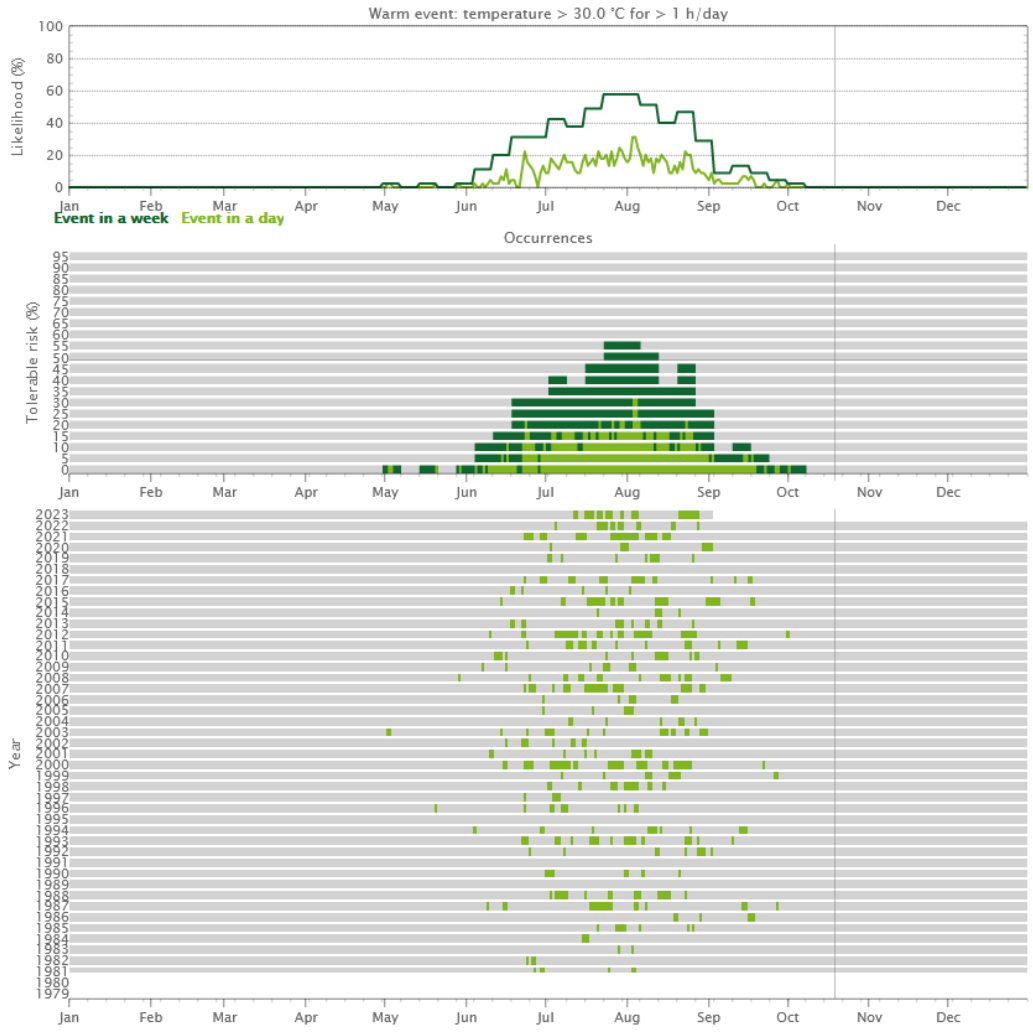

Figure 3. Assessment of the risk of heat waves within the Lulin residential area in the period 1979-2022 [27].

2.2. Approach and methods for SUHI Intensity calculation

This study proposes an approach to investigate the intensity of SUHI in a local aspect and with a pragmatic focus: providing an adequate spatial information base for urban planning and management purposes, and the transformation of urban areas towards a more sustainable development pattern. Through this term, we mean a scientifically based readiness to adapt effectively to environmental (climate change) and societal dynamic variables (societal needs, access to resources, land use priorities).

The need for precise spatial information provides a rationale to undertake a study of SUHI intensity at a local scale as a direct reflection of the spatial combinations of environmental components and their thermal characteristics in a specific urban location or smaller spatial urban unit (in this case, a residential area). This condition requires the provision of high spatial resolution data that allows for effective delineation (spatially-topologically and semantically) the main land cover types together with the thermal characteristics of the individual components that are forming and characterizing them. This means that the classical calculation approach could be transformed and interpreted as the difference between the temperature of each urban location within the studied urban space (housing complex) and the average minimum temperature of the land cover class with the lowest surface temperatures, in this same space:

$$SUHI=\Delta Tmin\text{-}n= Tn\text{-}TaverMIN,$$

-Tn - temperature at the given location,

Preprints (www.preprints.org) | NOT PEER-REVIEWED | Posted: 8 January 2024 doi:10.20944/preprints202401.0613.v1

-TaverMIN - average minimum land cover class temperature with minimum value.

This approach allows to assess the degree of intensity of SUHI more effectively:

(1) within each specific part of an urban area or spatial urban unit,

(2) provides information on the thermal load of individual land cover types

$$SUHI=\Delta Tmin\text{-}n= Tn\text{-}TaverMIN$$

(3) the thermal load at different spatial combinations of land cover types.

To implement this approach, it is first necessary to provide comprehensive continuum spatial information on surface temperature that reflects the spatial structure of the area in as much detail as possible. From a technological point of view, this is made possible by the use of thermal photogrammetry, which integrates digital photogrammetry with thermal imaging through the SfM (structure from motion) method.

For the aerial survey and the data collection, we have used the fixed-wing UAV model eBeeX produced by the company AgEagle Aerial Systems. This type of UAV is the only certified Class A2 platform that can fly over people as well as in situations beyond constant visual contact (BVLOS) (Figure 4a). To gather the necessary information, the platform is equipped with a specialized Duet T photogrammetric thermal sensor, combining a thermal Flir camera with a photogrammetric S.O.D.A. camera (Figure 4b). The sensor has a synchronized mechanism to perform and direct georeferencing of the capture, and a specially developed algorithm for integrated processing of the data from the two sensors. The use of the sensor results in data that allow, on the one hand, to reflect the geospatial and geometric characteristics of the environment, including its classification by different land cover classes, and, on the other hand, to obtain temperature data for each location within the surveyed area.

Figure 4. EbeeX fixed-wing UAS (a) and Duet T dual purpose thermal and mapping camera (b).

Another advantage of this UAV is the ability to orient the aerial images through GNSS in Real Time Kinematic (RTK) mode with high accuracy. As a result, the obtained images are georeferenced in the selected coordinate system. In this case, post-processing calculations for their orientation and use of pre-measured ground control points are not necessary. A CHCNAV GNSS system was used during the flights with a connection to a permanent GNSS network to obtain real-time corrections in image positions.

The intensity (magnitude) and temporal variability are of particular importance for the study of UHI and for taking measures to mitigate its effects. Urban heat island intensity is influenced by various physical and meteorological elements in the urban area, and there are limitations in calculating UHI variations within linear and two-dimensional analysis [28-31]. In general, the intensity measured in absolute values is more pronounced during the day when directed sun radiation creates significant differences between sealed, wet/dry, or vegetated surfaces, with flat surfaces such as roofs and streets particularly exposed. At night, the cooling process of these surfaces is significantly slower, with a significant inertia in the temperature after sunset, which in turn determines the occurrence of a relatively high UHI intensity. Given this, the present study was conducted over 4 consecutive days, under the conditions of a prolonged and deepening heat wave, during the period 11-14.07.2023, with all investigations conducted immediately after sunset, in the time interval 20:30-22:00. This allows to collect information that is not distorted by direct solar information and reflects the thermal characteristics of the different land cover types forming the urban area under study. Given the short time intervals suitable for collecting the required information and the capabilities of the selected UAV, the flights are pre-designed in dedicated software (E-motion

Preprints (www.preprints.org) | NOT PEER-REVIEWED | Posted: 8 January 2024 doi:10.20944/preprints202401.0613.v1

platform, Figure 5) to cover the required territory for the predefined time interval. For this purpose, four flight blocks have been designed for each of the days of the survey, each block including a territory to be flown within 90-minute intervals (approximately two flights per survey session). All flights are performed in automatic mode, which in turn makes it possible to repeat them with the same parameters, which can be used for data accumulation and continuous monitoring.

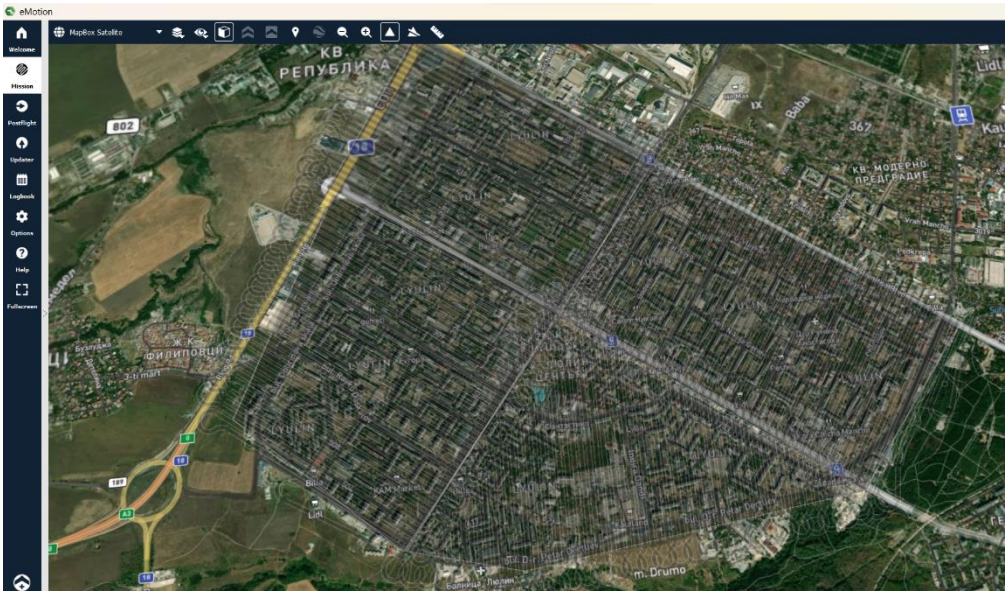

Figure 5. Screenshot from the flight mission planning platform E-motion.

A total of approximately 8561 images were collected, half of them containing temperature information as pixel values and the other half RGB values. These high-detail images were then processed using the photogrammetric software "Pix4D mapper" to generate high-precision thermal maps of the surveyed area. The final step of the processing involved calculating a thermal index for the surveyed area, resulting in a thermal raster map with improved spatial resolution based on the additional RGB images. The georeferenced raster data allowed for the application of statistical methods to extract temperature information for the area in more detail, as well as the application of zonal statistics for a more accurate assessment of the temperature emitted by different types of surfaces. The high spatial resolution of 10-20 cm/px provided the ability to determine the temperature of individual objects, leading to results not achievable with other types of data at this level.

3. Results

3.1. Geospatial and thermal characteristics of different land cover types explorations

A complete thermal survey and mapping of the residential area of Lyulin were performed for four consecutive days under the conditions of an ongoing heatwave: 11 - 14 July 2023. Digital geospatial layers with ground surface temperature data were generated as raster layers with a high spatial resolution of 5 cm/px. All data were collected in the period immediately after sunset, between 20:30 and 22:00 when the SUHI effect is most pronounced (Figure 6).

Preprints (www.preprints.org) | NOT PEER-REVIEWED | Posted: 8 January 2024 doi:10.20944/preprints202401.0613.v1

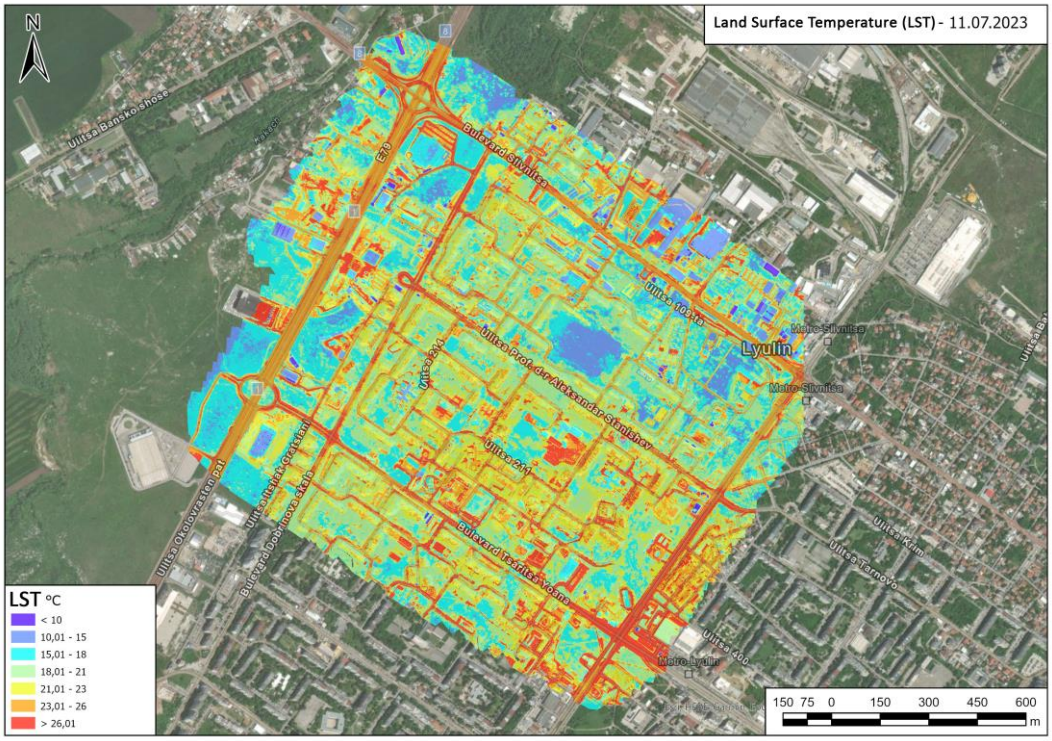

Figure 6. Thermal photography of the Lulin housing complex.

In order to establish the geospatial and thermal characteristics of the different land cover types, a classification based on a standard algorithm in the Pix4D mapper platform of the photogrammetrically captured 3D point cloud was performed, separating the main land cover types based on geometric and micrometric characteristics (Figure 7).

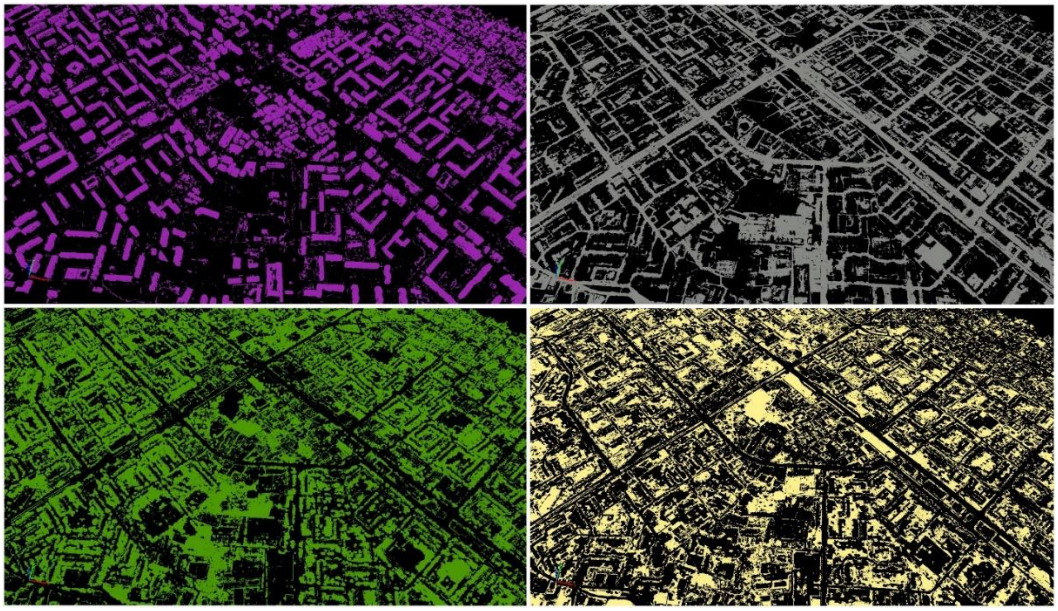

Figure 7. Classified point cloud: (top left) buildings; (top right) sealed surfaces; (bottom left) medium and tall vegetation; (bottom right) herbaceous vegetation.

The classified point cloud was processed in a GIS environment. To perform statistical analysis, the data type was transformed from a typical point cloud format (.las) to a raster model (.tiff) and subsequently vectorized into a vector polygon layer carrying information about the type of post-glacial surface within the study area (Figure 8).

Preprints (www.preprints.org) | NOT PEER-REVIEWED | Posted: 8 January 2024 doi:10.20944/preprints202401.0613.v1

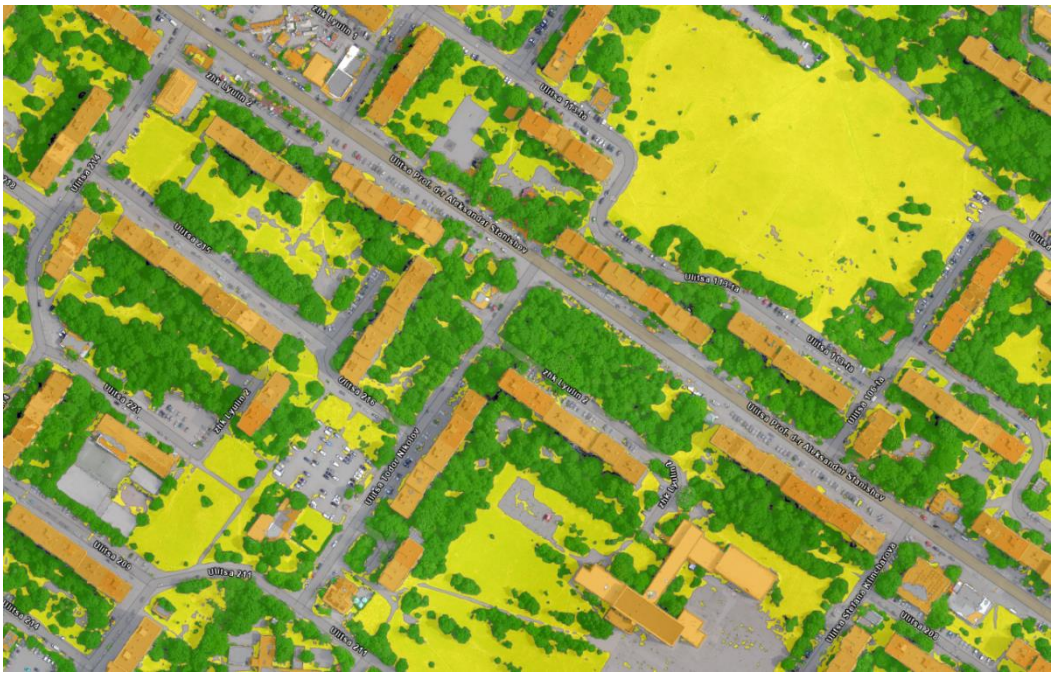

Figure 8. Vectorized polygon layer with information on surface types: yellow - grassy; green – medium and tall vegetation; orange - buildings; grey - impervious surface.

To calculate the mean temperature across the different surface types in the ArcGIS Pro software environment, Zonal Statistics as Table (Spatial Analyst) was implemented, which summarizes the raster values within the zones of another dataset and reports the results as a table (Figure 9). For this purpose, the operation was performed four times for the four separate days of thermal imaging. The raster data from the thermal imaging and zonal boundaries of different surfaces obtained by classifying the point cloud were used to perform the process.

=

Rowid	VALUE	COUNT	AREA	MIN	MAX	MEAN
1	0	5	5	0	2	0.6
2	1	5	5	0	3	1
3	2	3	3	1	2	1.667
4	4	1	1	3	3	3

Figure 9. Principle of performing zonal statistics in ArcGIS Pro Zonal Statistics as Table (Spatial Analyst).

Based on this process, statistically calculated values for the mean, standard deviation, and median of the land surface temperature at the boundaries of individual surfaces were obtained for each of the thermal imaging days (Table 1).

Table 1. Statistical information on the mean, standard deviation and median temperature of the different land surface types over the four measurement days.

 doi:10.20944/preprints202401.0613.v1

Day 1			
Land cover	**Mean**	**STD**	**Median**
Impervious surface	24,46	2,92	24,80
Buildings	20,55	4,00	21,08
Medium and high vegetation	20,02	1,91	20,12
Herbaceous vegetation	18,59	2,96	18,23
Day 2			
Land cover	**Mean**	**STD**	**Median**
Impervious surface	25,61	3,05	25,74
Buildings	22,58	3,61	22,84
Medium and high vegetation	21,17	2,39	21,45
Herbaceous vegetation	19,14	3,42	18,73
Day 3			
Land cover	**Mean**	**STD**	**Median**
Impervious surface	29,69	3,39	29,76
Buildings	26,91	4,09	27,02
Medium and high vegetation	25,00	2,48	24,99
Herbaceous vegetation	23,71	3,48	23,30
Day 4			
Land cover	**Mean**	**STD**	**Median**
Sealed surface	26,93	3,27	27,07
Buildings	22,96	3,39	22,96
Medium and high vegetation	21,29	1,88	21,10
Herbaceous vegetation	21,02	3,03	20,76

The data are also presented in a graph (Figure 10) for a clearer visualization of the degree of heating of the different surfaces as well as the temperature differences on the same surface over the four days.

Preprints (www.preprints.org) | NOT PEER-REVIEWED | Posted: 8 January 2024 doi:10.20944/preprints202401.0613.v1

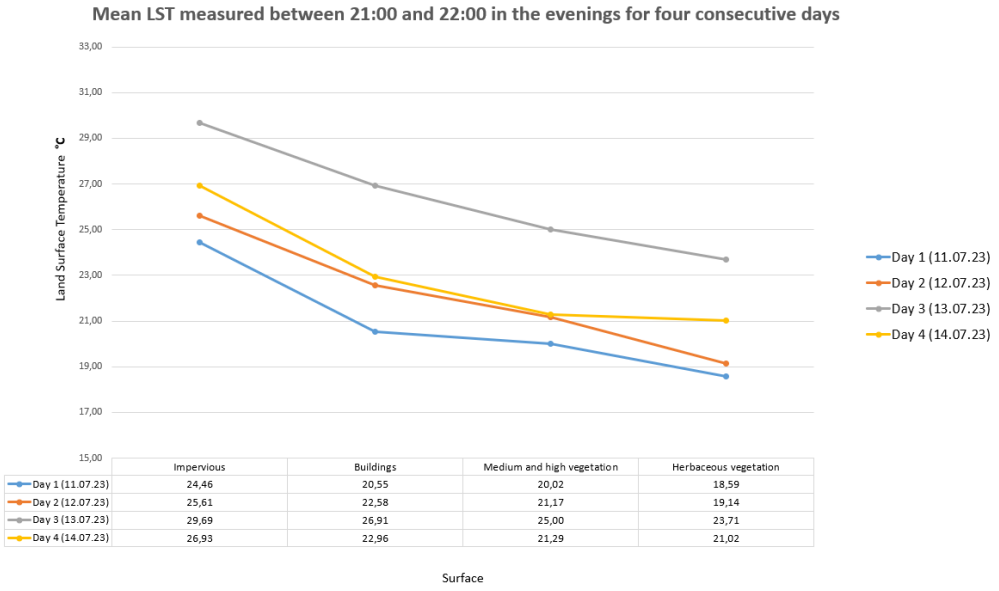

	Impervious	Buildings	Medium and high vegetation	Herbaceous vegetation
Day 1 (11.07.23)	24,46	20,55	20,02	18,59
Day 2 (12.07.23)	25,61	22,58	21,17	19,14
Day 3 (13.07.23)	29,69	26,91	25,00	23,71
Day 4 (14.07.23)	26,93	22,96	21,29	21,02

Figure 10. Average temperature for different surface types measured on four consecutive days between 21:00 and 22:00.

In the results presented in graphical form, it can be seen that although these are consecutive days and the warmest in the selected period, there are differences in the mean temperatures for the same surface types. The third day, 12 July 2023, is identified as the warmest of the four days. The gradual increase in surface temperatures during the first two days is impressive, reaching their highest values in the period of the recording in the evening hours of the third day and weakening in the evening hours of the fourth day, which marks the start of the beginning of the cooling (passing of the heat wave). The graph clearly shows the correlation of the highest averaged values for the land cover types with the sealed surfaces and the lowest values found in the areas mainly occupied by herbaceous vegetation.

3.2. Calculation of local SUHI intensity

For this study, a local SUHI intensity approach has been applied to individual urban units. It is expressed as the difference between the temperature in the relevant part of the urban area and the average minimum temperature of the land cover class that is natural and has the lowest surface temperature values. On this basis, for each of the days of thermal imaging, the parts with minimum temperatures have been separated and averaged for that day (Table 2).

Table 2. Average land surface temperature in non-urban areas for different days of thermal survey.

Day 1 (11.07.23)	Day 2 (12.07.23)	Day 3 (13.07.23)	Day 4 (14.07.23)
15 °C	**15,5 °C**	**17,5 °C**	**16 °C**

A magnitude was calculated for each of the pixels in the thermal map of the area using the formula presented in the methodological background in Section 2.2. This model (Figure 11) clearly shows a concentration of high-intensity areas within the central area and along the main boulevards in the area, where there is a significant concentration of sealed artificial surfaces.

Preprints (www.preprints.org) | NOT PEER-REVIEWED | Posted: 8 January 2024 doi:10.20944/preprints202401.0613.v1

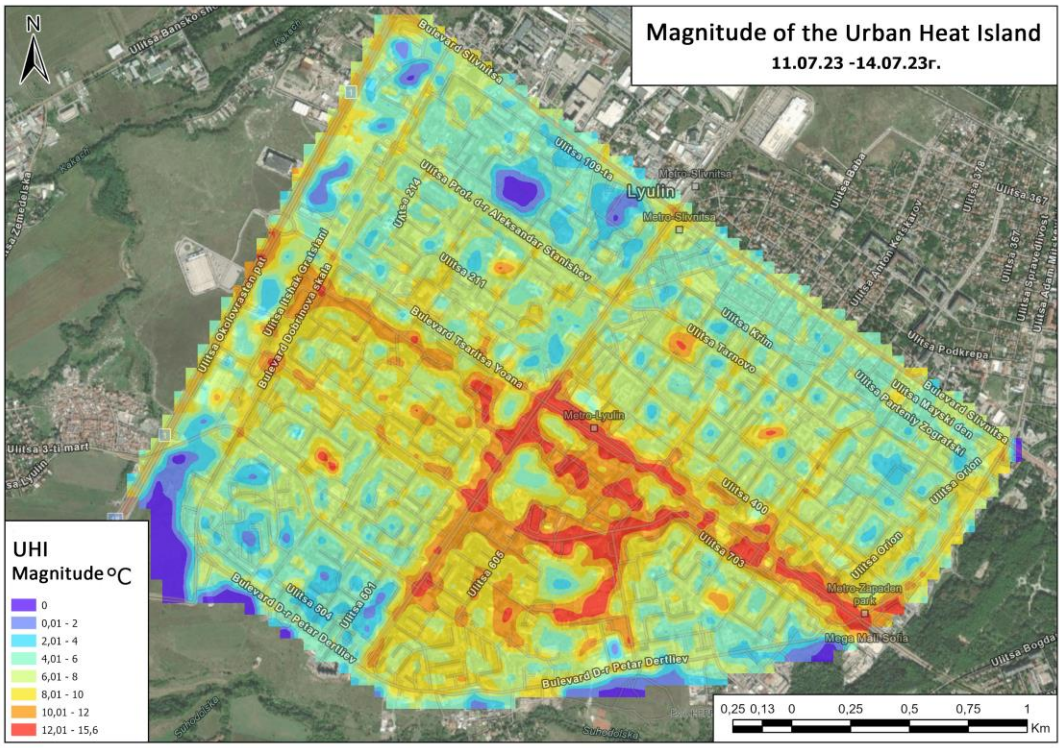

Figure 11. Magnitude map of an UHI within the boundaries of a housing complex Lulin for the period 11- 14 July 2023.

Land surface temperature values during the study period in these areas reached up to 16 °C higher than those outside urban areas. Areas that are not in close proximity to major boulevards (in this case, Tsaritsa Ioana Boulevard) and wide sealed areas have lower magnitude and therefore temperature values much closer to those measured outside the urban area (up to 2-4 °C difference). Transition zones between those with a low proportion of sealed, unnatural surfaces and those with a high proportion of artificial surfaces have 5 - 8 °C higher land surface temperatures relative to those measured outside urban areas.

To more clearly represent some of the morphological features of these areas with differences in SUHI intensity, several fragments with a higher level of detail and spatial resolution have been prepared (Figure 12 a, b, c).

Figure 12. a. UHI intensity in areas dominated by sealed artificial surfaces.

Preprints (www.preprints.org) | NOT PEER-REVIEWED | Posted: 8 January 2024 doi:10.20944/preprints202401.0613.v1

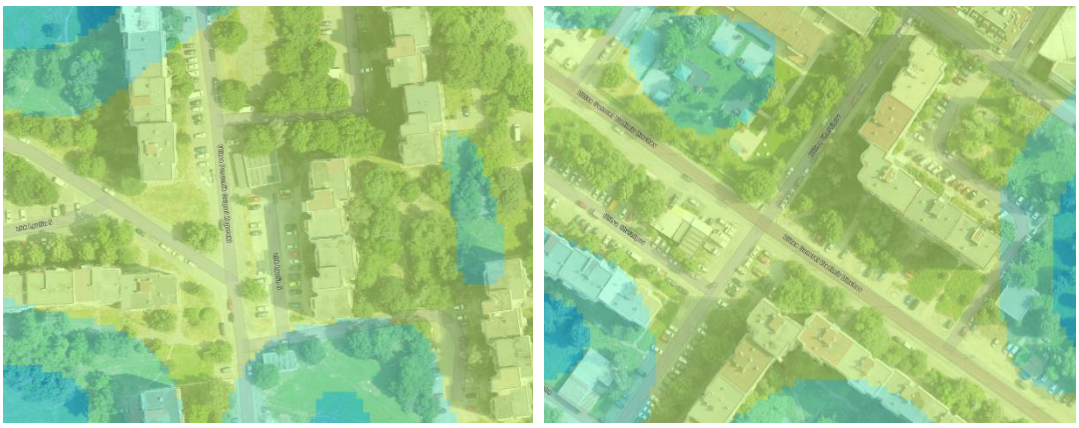

Figure 12. b. Areas with an even ratio of sealed and natural surface types.

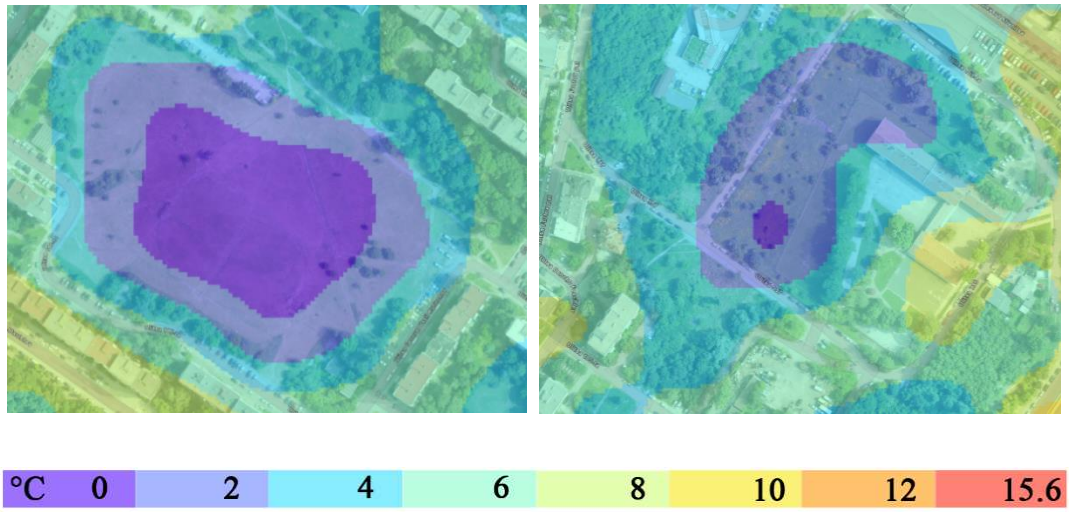

Figure 12. c. Areas with a predominant proportion of natural surface types.

4. Discussion

The UHI is a complex geospatial phenomenon of urban climate, formed under the direct influence of urban morphostructure, dominant architectural solutions, and the functionality of urban space. The phenomenon manifests itself at different spatiotemporal scales. Remote sensing provides a new perspective to record the phenomenon at regional scales and facilitates discussions regarding urban climate thermal issues and their effects [32]. At the same time, taking rapid action in urban management to respond to SUHI requires information that is the result of accurate, instantaneous, observations with high spatial specificity for affected areas. The present study focuses specifically on the potential of integrating geospatial technologies and UAS-based thermal photogrammetry for registering SUHI at the micro and local level of providing such timely information to responsible parties in urban management and taking proactive and rapid measures to mitigate the effect with direct relevance to the health of residents and maintenance of important urban infrastructure systems.

Our results provide grounds to argue that the integrated approach allows us to correctly reflect the impact of environmental heterogeneity on the intensity of SUHI occurrence. We see strong potential for incorporating such research into systems for developing digital urban twining, which would raise a series of practically oriented questions around the design of cities to accelerate their climate adaptation. For example, observations on the manifestation of SUHI intensity concerning structural urban conditions and the characteristics of building types could be used to develop additional building indices and impute specific obligations to architectural and construction activities (including energy efficiency). The local registration of SUHI, its intensity under heatwave conditions,

Preprints (www.preprints.org) | NOT PEER-REVIEWED | Posted: 8 January 2024 doi:10.20944/preprints202401.0613.v1

and the analysis of the potential vulnerability of the location to future similar phenomena (structural prerequisites, adjacency of land cover types, location in the general urban fabric) allow a clear addressing of this vulnerability to the relevant properties of the cadastral register. The latter will greatly facilitate contact with the public and ensure public support for the implementation of appropriate mitigation measures.

Representing the characteristics of SUHI and its intra-urban variability in a form suitable for integration with others, e.g. socio-economic, information may be of defining importance for future interdisciplinary research and as a possible screening tool for policy making [33]. The conditions of use by urban planners and architects of new scientific data on environmental quality have been repeatedly discussed [34]. This stems from the lack of correspondence between the range of environmental phenomena and the spatial extent of urban units. In the context of the latter - pragmatically oriented scientific analyses and data specifically addressing areas of interest can serve this relationship and make new scientific data crucial for sustainable forms of urban planning. In the data presented for the residential area of Lyulin, it is evident that the highest magnitude of SUHI is observed in sectors with development densities above 80% at the contact of major transport arteries (with major importance for the center-periphery connection) and adjacent commercial facilities and open parking lots. An additional highly unfavorable factor is impervious spaces with a disturbed structure. The large number of open inter-block spaces in Lulin fails to help mitigate the effect.

a.

b.

Figure 13. Impervious areas (a) with disturbed surface structure (b) suitable for undertaking redevelopment and landscaping.

The approach and the results it generates provide an opportunity to undertake a series of discussions and comparative analysis of information at different spatial scales of urban areas: for example, the relationship between (1) SUHI effect data in relation to the type of local climate zones and (2) SUHI effect data concerning the local heterogeneity of the relevant urban location. While the first type of data is well suited for discussing general principles in urban design decisions for adapting urban development plans to climate change, the second type of data provides a direct basis for discussing their important details - material and cover types, building spacing, building heights and their adjacencies, participation of green elements.

SUHI methodology, its accuracy, and operational feasibility are of fundamental importance for monitoring the phenomenon [35]. The calculation approach proposed here is an interpretation of the traditional approach focusing on the precision of the results with emphasis on the intensity of the phenomenon and its specific spatial parameters of occurrence. The results of applying such an approach are conducive to a discussion of the relationship between SUHI magnitude with urban development patterns and geographically specific combinations of land cover types. Of particular interest would be an analysis of the manifestation of SUHI in urban areas where there are active contemporary variables - population growth, overdevelopment and the emergence of new public facilities, increased traffic congestion, etc., which are also emphasized in the test area. The latter gives us a reason to point out the objective necessity of reorientation of the urban model of Sofia

Municipality, and in particular of the Lyulin district, towards a more sustainable and adequate to the new geographical environment perspective.

5. Conclusions

The integration of geospatial technologies and UAS-based thermal photogrammetry for mapping and assessment of the SUHI provides information with high accuracy and spatial correctness about the intensity of the phenomenon. The approach has a high potential for tracking thermal urban issues at local and micro scales.

Data from a test of the approach in a heat wave period in the largest and relatively self-contained urban unit, a residential area of the Bulgarian capital and Bulgaria, confirm that this methodology allows to correctly reflect the influence of environmental heterogeneity on the intensity of the SUHI manifestation.

This information base is very favorable for combining with other information from the functioning of the urban structure and systems - social, economic, and service (in energy and transport) to define both effective short-term measures (to mitigate thermal stress during a heat wave) and long-term strategic measures to establish urban patterns resilient to the changing geographical environment.

Author Contributions: Conceptualization, SD; methodology, S.D. M.I.; software, M.I.; validation, B.B., L.S. and S.P.; formal analysis, S.D., B.B., M.I., L.S., S.P; writing—original draft preparation, S.D., B.B., M.I., L.S., S.P.; writing—review and editing, S.D., B.B., L.S.; visualization, M.I.; All authors have read and agreed to the published version of the manuscript

Funding: This research was funded by the European Union - NextGenerationEU, through the National Recovery and Resilience Plan of the Republic of Bulgaria, project No BG-RRP-2.004-0008-C01.

Conflicts of Interest: The authors declare no conflicts of interest.

References

1. Nuissl, H., Siedentop, S. Urbanisation and Land Use Change. In: Weith, T., Barkmann, T., Gaasch, N., Rogga, S., Strauß, C., Zscheischler, J. (eds) *Sustainable Land Management in a European Context. Human-Environment Interactions,* **2021**, Vol 8. Springer, Cham. https://doi.org/10.1007/978-3-030-50841-8_5
2. Yang Jun, Yuxin Yang, Dongqi Sun, Cui Jin, Xiangming Xiao, Influence of urban morphological characteristics on thermal environment, *Sustainable Cities and Society*, **2021**, Volume 72, 103045, ISSN 2210-6707, https://doi.org/10.1016/j.scs.2021.103045
3. Mills, G. Luke Howard and the climate of London. *Weather* **2008**, Vol. 63 (6), pp. 153-157
4. Zhou, B., D. Rybski, J.P. Kropp. The role of city size and urban form in the surface urban heat island, *Sci. Rep.*, **2017**, Vol. 7, p. 4791
5. Vásquez-Álvarez, P.E.; Flores-Vázquez, C.; Cobos-Torres, J.-C.; Cobos-Mora, S.L. Urban Heat Island Mitigation through Planned Simulation. *Sustainability* **2022**, Vol. 14, 8612. https://doi.org/10.3390/su14148612
6. Pacheco P, Mera E, Fuentes V. Intensive Urbanization, Urban Meteorology and Air Pollutants: Effects on the Temperature of a City in a Basin Geography. *Int J Environ Res Public Health*. **2023**, Vol. 20(5):3941. doi: 10.3390/ijerph20053941. PMID: 36900952; PMCID: PMC10001953.
7. Constantinescu D., Cheval, S., Caracaş, G., Dumitrescu, A. Effective monitoring and warning of Urban Heat Island effect on the indoor thermal risk in Bucharest (Romania) *Energ. Buildings,* **2016,** Vol. 127, pp. 452-468
8. Li, X.; Zhou, Y.; Asrar, G.R.; Imhoff, M.; Li, X. The surface urban heat island response to urban expansion: A panel analysis for the conterminous United States. *Sci. Total Environ.* **2017**, pp. 605–606, 426–435
9. Li Xiaoma, Yuyu Zhou, Sha Yu, Gensuo Jia, Huidong Li, Wenliang Li, Urban heat island impacts on building energy consumption: A review of approaches and findings, *Energy*, **2019**, Volume 174, Pages 407-419, ISSN 0360-5442, https://doi.org/10.1016/j.energy.2019.02.183
10. Zhou Y., Weng, Q., Gurney, K.R., Shuai, Y., Hu, X.Estimation of the relationship between remotely sensed anthropogenic heat discharge and building energy use, ISPRS J. Photogramm. *Remote Sens.*, **2012**, Vol. 67, pp. 65-72
11. Zhao, L. et al. Interactions between urban heat islands and heat waves. *Environ. Res. Lett.*, **2018.** Vol. 13, 034003.
12. Chapman, S., Watson, J. E. M., Salazar, A., Thatcher, M. & McAlpine, C. A. The impact of urbanization and climate change on urban temperatures: a systematic review. *Landsc. Ecol.*, **2017.** Vol. 32, 1921–1935.
13. Heaviside, C., Macintyre, H. & Vardoulakis, S. The urban heat island: implications for health in a changing environment. *Curr. Environ. Health*, **2017**, Rep. 4, 296–305.

14. Estrada, F., Botzen, W. W. & Tol, R. S. A global economic assessment of city policies to reduce climate change impacts. *Nat. Clim. Chang*., **2017**, Vol. 7, 403.
15. Li, Y., Schubert, S., Kropp, J.P. et al. On the influence of density and morphology on the Urban Heat Island intensity. *Nat Commun*, **2020**, Vol. 11, 2647. https://doi.org/10.1038/s41467-020-16461-9
16. Oke T.R. The distinction between canopy and boundary-layer urban heat islands, *Atmosphere,* **1976,** *Vol.* 14:4, 268-277, DOI: 10.1080/00046973.1976.9648422
17. Huang, K.; Li, X.; Liu, X.; Seto, K.C. Projecting global urban land expansion and heat island intensification through 2050. *Environ. Res. Lett.* **2019**, Vol. 14, 114037.
18. McDonnell M.J., I. MacGregor Fors. The ecological future of cities, *Science,* **2016**. Vol. 352, pp. 936-938.
19. Irfeey, A.M.M.; Chau, H.-W.; Sumaiya, M.M.F.; Wai, C.Y.; Muttil, N.; Jamei, E. Sustainable Mitigation Strategies for Urban Heat Island Effects in Urban Areas. *Sustainability* **2023**, Vol. *15*, 10767. https://doi.org/10.3390/su151410767
20. Almeida, C.R.d.; Teodoro, A.C.; Gonçalves, A. Study of the Urban Heat Island (UHI) Using Remote Sensing Data/Techniques: A Systematic Review. *Environments* **2021**, Vol. 8, 105. https://doi.org/10.3390/environments8100105
21. Alves E., M. Anjos, E. Galvani. Surface urban heat island in middle city: spatial and temporal characteristics. *Urban Sci.* **2020**, Vol. 4 (4), p. 54, 10.3390/urbansci4040054
22. Stewart I.D., E.S. Krayenhoff, J.A. Voogt, J.A. Lachapelle, M.A. Allen, A.M. Broadbent Time evolution of the surface urban heat Island. e2021EF002178. *Earth's Fut.*, **2021**. Vol. 9 (10), 10.1029/2021EF002178
23. Dimitrov, S.; Popov, A.; Iliev, M. An Application of the LCZ Approach in Surface Urban Heat Island Mapping in Sofia, Bulgaria. *Atmosphere* **2021**, Vol. 12, 1370. https://doi.org/10.3390/atmos12111370
24. Geodesy, Cartography and Cadastre Agency. Republic of Bulgaria. Available online: https://www.cadastre.bg/en/frontpage (accessed on December 2023).
25. Dimitrov S., Popov, A., Iliev, M. "Mapping and assessment of urban heat island effects in the city of Sofia, Bulgaria through integrated application of remote sensing, unmanned aerial systems (UAS) and GIS", Proc. SPIE 11524, In Proceedings of the Eighth International Conference on Remote Sensing and Geoinformation of the Environment (RSCy2020), 115241A (26 August 2020); https://doi.org/10.1117/12.2571967
26. Comprehensive Programme for Improvement of Ambient Air Quality of Sofia Municipality for the period 2021 - 2026, adopted by Decision No 204/22.04.2021 of the Sofia Municipal Council, Sofia Municipality, (5 November 2022) https://www.sofia.bg/en/components-environment-air
27. Meteoblue. Weather forecast data. Available online: http://www.meteoblue.com (accessed on December 2023)
28. Demuzere, M., Harshan, S., Järvi, L., Roth, M., Grimmond, C.S.B., Masson, V., Oleson, K.W., Velasco, E. and Wouters, H., Impact of urban canopy models and external parameters on the modelled urban energy balance in a tropical city. Q.J.R. *Meteorol. Soc.,* **2017**, 143: 1581-1596. https://doi.org/10.1002/qj.3028
29. Groleau, D., Mestayer, P.G. Urban Morphology Influence on Urban Albedo: A Revisit with the Solene Model. Boundary-Layer *Meteorol*, **2013**. Vol. 147, 301–327, https://doi.org/10.1007/s10546-012-9786-6
30. Oke, T. R. The urban energy balance. *Progress in Physical Geography: Earth and Environment*, **1988**, Vol. 12(4), 471-508. https://doi.org/10.1177/030913338801200401
31. Yong Xu, Chao Ren, Peifeng Ma, Justin Ho, Weiwen Wang, Kevin Ka-Lun Lau, Hui Lin, Edward Ng. Urban morphology detection and computation for urban climate research, *Landscape and Urban Planning*, **2017**. Volume 167, Pages 212-224, ISSN 0169-2046, https://doi.org/10.1016/j.landurbplan.2017.06.018.
32. Zhou Yi, Haile Zhao, Sicheng Mao, Guoliang Zhang, Yulin Jin, Yuchao Luo, Wei Huo, Zhihua Pan, Pingli An, Fei Lun, Exploring surface urban heat island (SUHI) intensity and its implications based on urban 3D neighborhood metrics: An investigation of 57 Chinese cities, *Science of The Total Environment*, **2022**, Volume 847, 157662, ISSN 0048-9697, https://doi.org/10.1016/j.scitotenv.2022.157662 .
33. Chakraborty T., Hsu, A., Manya, D., Sheriff, G. A spatially explicit surface urban heat island database for the United States: Characterization, uncertainties, and possible applications, *ISPRS Journal of Photogrammetry and Remote Sensing*, **2020**, Volume 168, Pages 74-88, ISSN 0924-2716, https://doi.org/10.1016/j.isprsjprs.2020.07.021
34. Panagopoulos Th, Duque, J. A. G., Dan, M.B., Urban planning with respect to environmental quality and human well-being, *Environmental Pollution*, **2016**, Volume 208, Part A, Pages 137-144, ISSN 0269-7491, https://doi.org/10.1016/j.envpol.2015.07.038
35. Zhang W., Li, Y., Zheng, C., Zhu, Y. Surface urban heat island effect and its driving factors for all the cities in China: Based on a new batch processing method, *Ecological Indicators*, **2023**. Volume 146, 109818, ISSN 1470-160X, https://doi.org/10.1016/j.ecolind.2022.109818